

Universal resonant ultracold molecular scattering

Vladimir Roudnev and Michael Cavagnero

Department of Physics and Astronomy, University of Kentucky, Lexington, KY 40506-0055

The elastic scattering amplitudes of indistinguishable, bosonic, strongly-polar molecules possess near-threshold resonance features that can be tuned with an applied electric field. An adiabatic description of ultracold collisions of field-aligned molecules provides an elementary and complete interpretation and classification of these resonant states; including three series of threshold bound states, shape resonances, and mixed Feshbach/shape resonances. Small tunneling amplitudes for the resonant states result in strong correlations between the magnitude of total elastic cross sections and the isotropy, or lack thereof, of threshold differential cross-sections. Implications of universal scaling for the formation and trapping of dilute quantum degenerate gases are discussed. PACS numbers: 34.50.Cx, 31.15.ap, 33.15.-e, 34.20.-b

One might naturally expect that as dilute polar gases are cooled toward the absolute zero of temperature, a regime should emerge in which only the longest ranged forces – dipole-dipole interactions – are relevant; in which case different polar gases would share a universal equation of state. Recent theoretical investigations of molecular collisions, however, have identified universal characteristics only in the temperature regime of semi-classical collision dynamics [1]. One purpose of this Letter is to articulate the reasons why, and to suggest how universal properties might emerge at the lowest temperatures where collective phenomena associated with quantum degeneracy are expected [2, 3].

Of particular interest are the properties of near-threshold resonances which have appeared in calculations of RbCs and SrO scattering [4, 5]. A second purpose of this Letter is to provide a complete classification and interpretation of these resonances, and to demonstrate their relevance to virtually all strongly polar molecules.

Many molecules possess polar charge distributions in their lowest electronic energy states. However, in the absence of external fields, as a consequence of parity conservation, even strongly “polar” molecules have no net dipole moment. Interactions between colliding molecules induce a transient polarization in the absence of external fields, though this produces a relatively benign and isotropic ($1/r^6$) van der Waals attraction at large intermolecular separations. The stronger ($1/r^3$) *anisotropic* interactions of interest here require an external electric field, $\vec{\mathcal{E}}$, coupling opposite parity states, and producing a generally field-dependent dipole moment $\vec{\mu}(\mathcal{E}) = -(dE/d\mathcal{E})\vec{\mathcal{E}}$ for all molecules [5].

The magnitude and sign of the “induced” dipole moment, μ , depends on details of the $E(\mathcal{E})$ Stark shift of the state of interest for a given molecule. In a field-free region, two molecular states of opposite parity are separated by an energy gap, so that $E(\mathcal{E})$ varies quadratically for small fields. At larger fields, Stark maps tend to a linear regime, yielding a maximal induced dipole moment $\vec{\mu} \rightarrow \vec{d} = qsd\hat{d}$, where q is an effective charge, and where s is a measure of the charge separation along the field axis, typically a few Bohr in size. The magnitude of the electric

field required to maximize the dipole moment μ depends on the size of the zero-field energy gap; molecules in Π or Δ states can have quite small gaps (owing to Λ -doubling), producing maximal dipole moments with modest fields, while those with ground Σ states tend to have relatively large gaps requiring larger fields.

At intermolecular separations much greater than the charge displacement, $r \gg s$, molecular interactions reduce to the familiar dipole-dipole form

$$V(\vec{r}) = \frac{d^2}{r^3} \left[\hat{d}_1 \cdot \hat{d}_2 - 3(\hat{r} \cdot \hat{d}_1)(\hat{r} \cdot \hat{d}_2) \right] \quad (1)$$

which, for a pair of identical molecules in the same field-aligned state, yields an equation of relative motion

$$\left[-\frac{\hbar^2}{2M} \nabla^2 + \frac{\mu^2}{r^3} (1 - 3(\hat{r} \cdot \hat{z})^2) \right] \psi(\vec{r}) = E_{\text{rel}} \psi(\vec{r}) \quad (2)$$

where \vec{r} is the intermolecular displacement, \hat{z} is the field axis and M is the reduced mass. μ assumes its maximal value of d at large fields, but reduces to zero as $\mathcal{E} \rightarrow 0$.

Equation (2) may be written in dimensionless form *independent of M and μ* if all distances and energies are measured in dipole units

$$D = \mu^2 M / \hbar^2, \quad E_D = \hbar^6 / (M^3 \mu^4) \quad (3)$$

The emergence of these field-dependent length and energy scales, previously noted by many authors [6], is striking when one recognizes that *for maximal μ* , $D \sim 10^2 - 10^5$ times *larger* than typical molecular length scales, while $E_D \sim 10^{-4} - 10^{-12}$ times *smaller* than typical rotational level splittings. A final purpose of this Letter is to demonstrate how these dipole scales are manifested in the ultracold collisions of all polar systems.

There are two restrictions on the domain of validity of Eq. (2). The dipole-dipole interaction accurately represents the intermolecular potential only where higher multipoles and exchange terms are negligible. Within an exchange radius, $r < r_e \sim 20 - 30$ Bohr, intermolecular interactions are complex and species-dependent. There is also a range of separations at which the fields created

by the dipoles dominate the external field, so that effects of collisional depolarization become important for $r < r_c \sim (d/\mathcal{E})^{1/3}$, typically ~ 100 Bohr in moderate fields for strongly polar molecules. Key to the present study is that both of these length scales are orders of magnitude smaller than D , especially as $\mu \rightarrow d$.

Propagation of waves from r_c throughout the range of the dipole-dipole potential amplifies species-dependent short-range contributions to scattering, which can in principle be represented by a short-range reaction matrix [6]. Here, this sensitivity is illustrated by simply representing short-range physics with an impenetrable hard-sphere at $r = r_0$. Variations in r_0 then represent the effects of alternative short-range species-dependent interactions. More refined techniques for representing short-range physics are available, but unnecessary for our purposes.

Since most analyses to date have emphasized scattering properties over a broad temperature range [7], and since it is known from the study of threshold laws that many partial waves contribute to dipole scattering (even near zero energy) [8], Eq. 2 is usually analyzed by partial wave expansion. In contrast, we adopt here Born-Oppenheimer adiabatic states, whose eigenenergies relevant to bosonic molecules are displayed in dipolar units in Fig. 1. The potential curves and coupling matrix elements of this representation are *universal* (i.e. independent of collision partner, reduced mass, dipole moment, and electric field strength) for all r beyond r_0 . Note that r_0 can be $\sim 10^{-3}$ dipole units or smaller for many systems. Fig. 1 shows that an infinity of channels (corresponding to the infinity of partial waves) produce a single attractive potential, $V_{0,0}$, and an infinite number of potentials with centrifugal barriers.

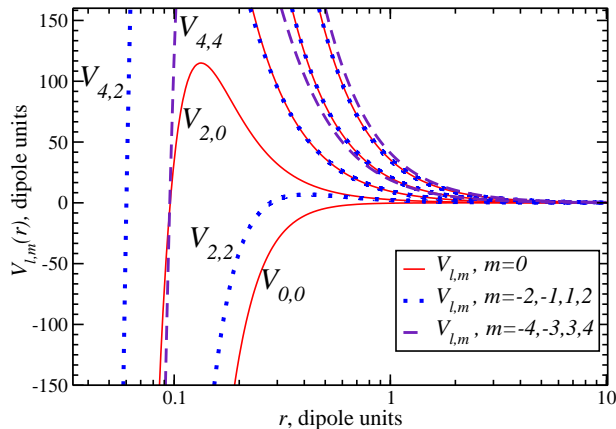


FIG. 1: (Color online) Adiabatic potential curves for bosonic polar molecules. The curves are labeled by their asymptotic angular momentum ℓ and by their exact magnetic quantum number m .

Due to cylindrical symmetry about the field axis, the adiabatic states couple only to other states of the same

N channels	$r_0 = 0.01455$ d.u.		$r_0 = 0.01457$ d.u.		$r_0 = 0.01548$ d.u.	
	<i>ad.</i>	<i>p.w.</i>	<i>ad.</i>	<i>p.w.</i>	<i>ad.</i>	<i>p.w.</i>
1	12.46	0.005	11.16	0.005	0.47	0.006
2	35.16	73.86	30.87	65.85	2.28	3.77
3	4.34	3.49	411.51	3.32	2.55	8.30
4	3.94	16.50	505.75	15.14	2.63	2.89
5	4.08	26.54	416.25	24.07	2.66	2.68
8	4.13	2.79	409.63	20196.	2.69	2.70
16	4.14	3.87	409.64	306.02	2.71	2.71

TABLE I: Convergence of the elastic cross section with respect to the number of channels for the incident energy of $E = 10^{-3}$ d.u. . Results for adiabatic (*ad.*) and partial wave (*p.w.*) representations are shown. The adiabatic representation demonstrates much faster convergence, especially in the vicinity of a resonance.

m , which is strictly conserved. The adiabatic curves approach familiar centrifugal potentials at large r , permitting them to be labeled by their large- r angular momentum quantum number, ℓ , as well. Accordingly, the curves in Fig. 1, and the resonant states they support, are uniquely designated by (ℓ, m) . (For $m \neq 0$, the channels are degenerate, and we refer to degenerate channels by their maximum m value for brevity.) Note that $V_{2,2}$ and $V_{2,0}$ present universal barriers of heights $\sim 5E_D$ and $115E_D$, respectively. Since m is conserved, the $V_{2,2}$ channel is not coupled to the $V_{0,0}$ channel, while $V_{2,0}$ and the ground state channel are strongly coupled. Accordingly, at energies much smaller than $115E_D$, scattering is dominated by the two lowest adiabatic channels, absent the resonance features discussed below.

We have solved the coupled-channel Schrödinger equation in the adiabatic representation numerically [9], propagating from r_0 to asymptotic distances $r \sim 500D$. Special care is required to extract the asymptotic scattering parameters owing to the slow ($1/r^2$) decline of derivative coupling matrix elements. The adiabatic basis gives a clear numerical advantage over partial wave analysis for ultra-low energy scattering. A comparison of the rate of convergence of the total cross section (averaged over the field direction) is displayed in Table I. The adiabatic representation converges rapidly even in the vicinity of threshold resonances, far superior to the partial wave basis.

The contribution of various channels to the total elastic cross-section for bosonic scattering (averaged over the electric-field direction), is shown in Fig. 2, for $r_0 = 0.0108$ dipole units. The uncoupled $V_{0,0}$ and $V_{2,2}$ channels dominate scattering below $115E_D$, as indicated above. Note, however, that detailed convergence of the cross-section (even at energies less than a nano-Kelvin) requires several adiabatic channels. Both the magnitude of the threshold cross section and the degree of convergence vary with the hard-sphere radius, as they are sensitive to resonance formation in the inner wells of excited potential curves.

This is illustrated in Fig. 3, where the field-averaged elastic cross section is plotted versus hard-sphere radius at the near-threshold energy, $E = 10^{-3} E_D$. Note that the threshold cross-section varies by 4-orders of magnitude, depending on the specific details of the short-range scattering.

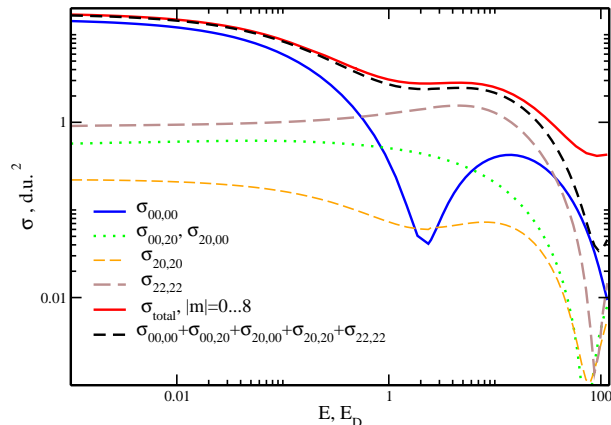


FIG. 2: (Color online) Channel contributions to the threshold cross section for $r_0 = 0.0108$ dipole units. The $(0,0)$ and 4 degenerate $(2,2)$ channels dominate scattering below $115 E_D$.

Figure 3 also illustrates the partial wave content of the scattering cross sections. The near-threshold cross section varies quasi-periodically with r_0 due to successive ‘‘Ramsauer minima’’ in the attractive adiabatic channel (i.e. varying r_0 alters the number of bound states in the ground state potential curve, and correspondingly sweeps the s-wave scattering length through complete cycles).

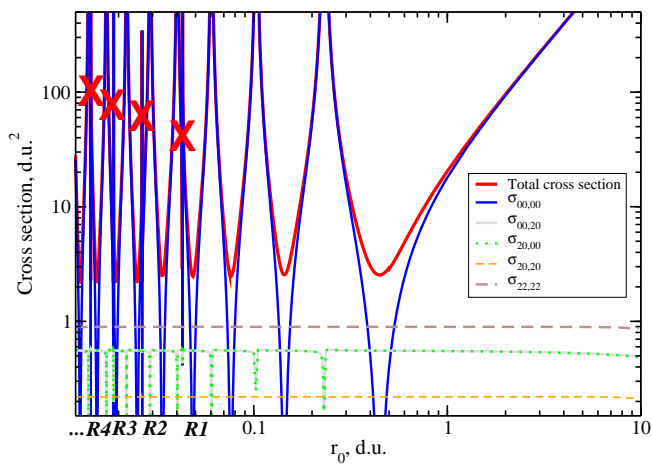


FIG. 3: (Color online) Near-threshold cross section as a function of the cut-off radius. Positions of the $(2,0)$ Feshbach-shape resonances are marked by **X**s and labeled as $R1$, $R2$, $R3$, $R4$.

The resonances shown in Fig. 3 can be predicted by semiclassical quantization in accurate fits to the potential curves. The positions of the successive Ramsauer

peaks in the $(0,0)$ potential are universally given (to 3 significant figures) by

$$r_0^{0,0}(n) = \frac{1}{4.37 + 3.46n + 0.675n^2} \quad (d.u.). \quad (4)$$

Similarly, the semiclassical description predicts positions of resonances in the $V_{2,0}$ potential that are marked as $R1$, $R2$, $R3$ etc. in Fig. 3, and given by

$$r_0^{2,0}(n) = \frac{1}{10.88 + 11.81n + 0.685n^2} \quad (d.u.). \quad (5)$$

If nonadiabatic coupling were negligible, these resonances would have a near-zero (tunneling) width when approaching threshold because of the large dipole-modified centrifugal barrier in Fig. 1. To the extent that tunneling is negligible, these are effectively discrete states coupled to the ground state continuum. Their actual width is due to decay into the lowest adiabatic channel through short-range nonadiabatic coupling. Accordingly, the $(2,0)$ resonances appear as Feshbach/Fano resonances in the total elastic cross section. Finally, there is also a series of extremely narrow tunneling resonances in the $V_{2,\pm 2}$ and $V_{2,\pm 1}$ potentials, whose positions are given by

$$r_0^{2,2}(n) = \frac{1}{1.14 + 7.07n + 0.685n^2} \quad (d.u.). \quad (6)$$

but these have little relevance to threshold elastic scattering, as the $m = 2$ channels are not coupled to the ground state channel.

We have not emphasized the energy dependence of these resonances here, but it is interesting to note that, for a fixed r_0 , the barrier heights of the $(2,0)$ and $(2,2)$ potential curves are at most sufficient to support a single resonance in each channel.

The dual Feshbach/shape nature of the $(2,0)$ resonance leads to strong correlation between the anisotropy of the differential cross section and the magnitude of the total cross section. One might expect strongly anisotropic scattering near a $(2,0)$ resonance. However, due to the small value of the tunneling amplitude, the inner well of the $(2,0)$ potential is only accessed through coupling to the $(0,0)$ channel. As illustrated in Fig. 4, anisotropy results only when the $(0,0)$ channel is ‘‘turned off’’ (either near a Ramsauer minimum or – due to interference – to the side of a Feshbach/shape resonance), and stems from long-range non-adiabatic coupling *outside* the $(2,0)$ potential barrier, as well as from the uncoupled $(2,\pm 2)$ and $(2,\pm 1)$ channels. As a result, whenever the scattering cross section peaks, the scattering becomes isotropic, even at the peak of the $(2,0)$ resonance. This view augments the interpretation of similar resonances in atomic collisions in very strong fields [10].

Sensitivity to r_0 indicates a corresponding sensitivity to short-range physics, and therefore, to the specific molecular species. However, following Ref. [5], variations

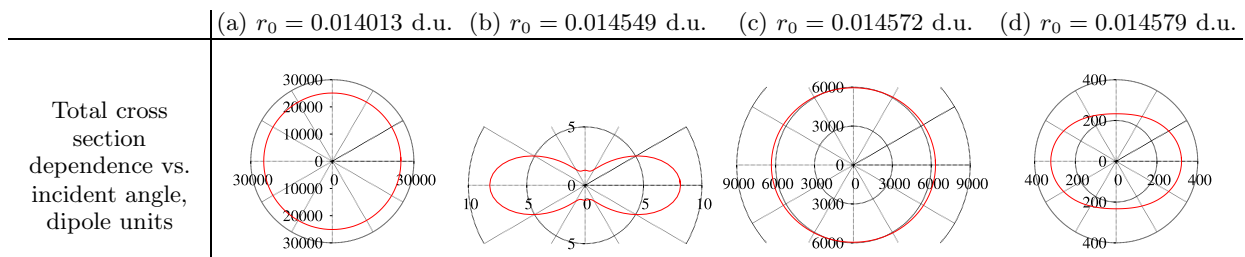


FIG. 4: (Color online) Cross section dependence on the angle between the incident direction and the field axis, for values of the cut off radius in the vicinity of the Feshbach/shape resonance. When the total cross section is large, the scattering is almost isotropic, even at the “d-wave” resonance, (c).

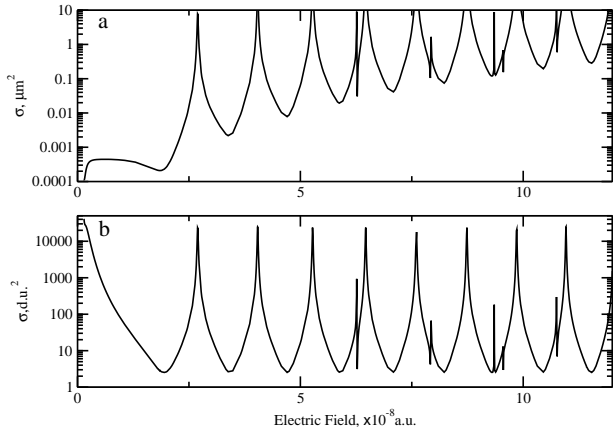


FIG. 5: Electric field dependence of the near-threshold KF elastic scattering cross section, in both (a) absolute and (b) dipole units. The minima of the cross section in the upper figure rise rapidly with the field as a result of rapidly growing dipole length.

in the electric field would permit such resonances to be observed in virtually all strongly polar molecules. We described above a dimensionless threshold cross section that varies with a dimensionless cut-off $\sigma_0[r_0(d.u.)]$. To the extent that short-range physics is insensitive to the external field, the observed elastic scattering cross section will scale with the field \mathcal{E} as $\sigma = D(\mathcal{E})^2 \sigma_0[r_0(a.u.)/D(\mathcal{E})]$, where $D(\mathcal{E})$ is given by Eq. 3. This field dependence is displayed in Fig. 5 for the KF molecule with $r_0 = 80$ a.u. chosen as short-range cut-off parameter, and assuming a quadratic field variation of the KF ground state. The cross-section is displayed in both conventional and in dipole units. Positions of successive peaks are readily predicted from Eqs. 4-6 and detailed knowledge of $\mu(\mathcal{E})$.

The adiabatic potential curves serve to identify $E < 115E_D$ as the universal energy range of ultracold molecular collisions, and $\sigma \sim 2D^2$ as the *minimum* elastic cross section for threshold collisions between polarized molecules, Fig. 5(b). Far greater cross sections $\sim 10^5 D^2$ are achievable with small variations of the applied field: note the micron² scale in Fig. 5(a). The dipole scales D

and E_D , and the resonances, have direct consequences for trapped ensembles, for which accurate calculations are now emerging [11]. Elastic scattering, as an aid to thermalization in evaporative cooling, will only improve as temperatures are lowered toward threshold, and can be increased dramatically with electric fields. If cooled at the low densities associated with the trapping of individual molecules on optical lattice sites [12], the relation of D to the optical wavelength will be a key parameter. On the other hand, at densities comparable to those of trapped atomic ensembles [13], fields can be used to vary D from less than to much larger than the mean distance between molecules, affording the possibility of tuning molecular gases from a “nearest neighbor” regime to one where every molecule interacts with every other molecule via the long-range dipole-dipole interaction.

The authors are grateful to John Bohn for helpful conversations and a critical reading of the manuscript.

-
- [1] C. Ticknor, Phys. Rev. Lett. **100**, 133202 (2008)
 - [2] J. Doyle, B. Friedrich, R. V. Krems, and F. Masnou-Seeuws, Eur. Phys. J. D **31**, 149 (2004)
 - [3] L. Santos, G. V. Shlyapnikov, P. Zoller, and M. Lewenstein, Phys. Rev. Lett. **85**, 1791 (2000)
 - [4] C. Ticknor and J. Bohn, Phys. Rev. A **72**, 032717 (2005)
 - [5] J. Bohn and C. Ticknor, in Proceedings of the XVII International Conference on Laser Spectroscopy, E. A. Hinds, A. Ferguson, E. Riis, eds., (World Scientific, 2005), p. 207.
 - [6] Bo Gao, J. Phys. B: At. Mol. Opt. Phys. **37**, L227 (2004)
 - [7] C. Ticknor, Phys. Rev. A **76**, 052703 (2007)
 - [8] H. Sadeghpour et. al., J. Phys. B. At. Mol. Opt. Phys. **33**, R93-R140 (2000)
 - [9] C. de Boor, B. Swartz, SIAM J. Numer. Anal., **10**, 582-606 (1973)
 - [10] Marinescu and L. You, Phys. Rev. Lett. **81**, 4596 (1998)
 - [11] K. Kanjilal and D. Blume, (private communication).
 - [12] S. Kotochigova and E. Tiesinga, Phys. Rev. A **73**, 041405 (2006)
 - [13] J. Stuhler, A. Griesmaier, T. Koch, M. Fattori, T. Pfau, S. Giovanazzi, P. Pedri, and L. Santos, Phys. Rev. Lett. **95**, 150406 (2005)